UKAEA-CCFE-PR(23)166

J. O. Allen, S. Desai, S. Freethy, K. Hawkins, M. A. Henderson, E. Kaijanen, C. Lechte, J. Lovell, E. Melidis, A. Munasinghe, J. Pearl, B. Plaum, A. Seidu, H. Webster, the MAST-U EBW Team

Design update of the MAST-Upgrade microwave heating and current drive system launchers

Design update of the MAST-Upgrade microwave heating and current drive system launchers

J. O. Allen, S. Desai, S. Freethy, K. Hawkins, M. A. Henderson, E. Kaijanen, C. Lechte, J. Lovell, E. Melidis, A. Munasinghe, J. Pearl, B. Plaum, A. Seidu, H. Webster, the MAST-U EBW Team

This is a preprint of a paper submitted for publication in
IEEE TRANSACTIONS ON PLASMA SCIENCE

Design Update on the MAST-Upgrade Microwave Heating and Current Drive System Launchers

Joe O. Allen[1], Shail Desai[1], Simon Freethy[1], Keith Hawkins[1], Mark A. Henderson[1], Carsten Lechte[2], James Lovell[1], Asanka Munasinghe[1], Jonathan Pearl[1], Burkhard Plaum[2], Helen Webster[1] and the MAST-U EBW Team

[1]UKAEA, Culham Science Centre, Abingdon, OX14 3DB, United Kingdom

[2]University of Stuttgart, IGVP, Pfaffenwaldring 31, 70569 Stuttgart, Germany

***Abstract*—MAST-Upgrade (MAST-U) is undergoing several enhancements to deliver increased performance and functionality. One such enhancement is the design, development, and implementation of an Electron Bernstein Wave (EBW) Heating and Current Drive (HCD) System. The MAST-U EBW System aims to provide experimental data for model validation, along with a greater understanding of EBW physics and its capabilities. The MAST-U EBW System will deliver up to 1.8 MW of microwave power via two microwave beams, at the dual frequencies of 28 GHz and 34.8 GHz for up to 4.5 s. This article provides an update on the system's in-vessel components, with particular focus on the quasi-optical launcher design and modelled performance.**

***Index Terms*—MAST-Upgrade, EBW, microwaves, heating, current drive, start-up**

I. Introduction

SEVERAL projects are underway to enhance the capability of MAST-Upgrade, one being the addition of an Electron Bernstein Wave (EBW) microwave Heating and Current Drive (HCD) system at 28 and 34.8 GHz. Two gyrotrons will produce a total of 1.8 MW of microwave power, with up to 1.6 MW delivered to the plasma due to transmission line losses. The two microwave beams are injected from the low-field side and coupled into the plasma via the two stage O-X-B mode conversion process. The MAST-U EBW project aims to provide experimental data relevant for the STEP HCD system, and other spherical tokamaks. See [1] for the physics and modelling driving the design and [2], [3] for engineering overviews of the system.

II. Quasi-optical launchers

Meeting project requirements necessitates a variety of launch options: On- and off-axis current drive, co- and counter-current drive, balanced co- and counter-current injection for pure heating. In order to optimise the microwave-plasma coupling the beams should be steerable in a toroidal and poloidal window around the optimum injection vector. In addition, the system should provide microwave assisted start-up capability. Balanced co- and counter-current injection (zero net current) is most straightforward to achieve by launching beams from the midplane of MAST-U, one directed upwards to drive current parallel to the plasma current and the other directed below the midplane (in opposite toroidal directions) to drive current anti-parallel to the plasma current.

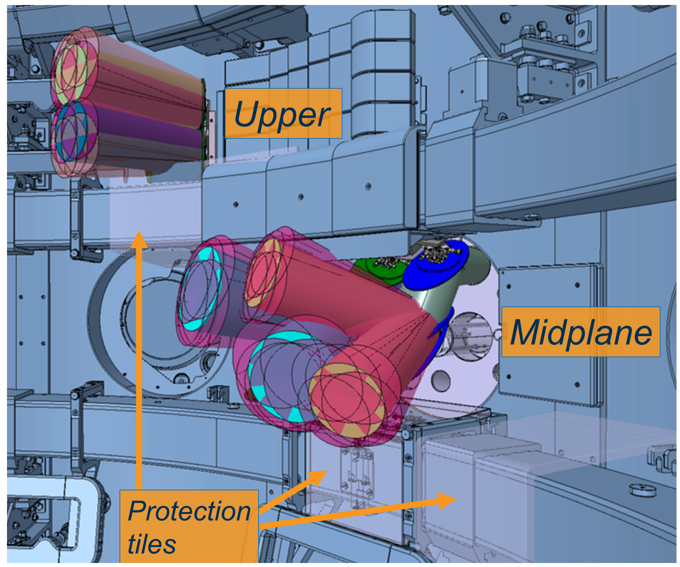

Fig. 1. Midplane and upper launcher models showing injected beam paths for a range of plasma scenarios and steering angles. Solid cones indicate the nominal injected direction, which are surrounded by translucent cones describing the extremities of a given mirror's steering range. Midplane mirrors are visible in green (delta) and blue (epsilon) and an example mounting bracket is included. Only the upper steering mirrors can be seen as the rest are either hidden by the beam cones or not visible. Orange arrows direct the reader to faintly visible L-shaped graphite protection plates for scattering uncoupled microwave power, discussed in section IV.

Additional midplane launcher steering covers a range of plasma scenarios in both the co- and counter-current directions. Microwave-plasma coupling through the O-X-B conversion process is strongly influenced by the divergence on the O-mode beam injected into the plasma. In general, the larger the Gaussian beam waist (the narrowest radius the beam is focused to) the lower the divergence of the beam, resulting in greater coupling efficiency [1]. An in-vessel view of the midplane and upper EBW launchers (on- and off-axis) is shown in figure 1, with mirrors depicted in blue and green and including the beam envelopes and steering ranges into the plasma.

A. On-axis / Midplane launcher

To deliver pure heating (balanced current drive), we have designed two midplane quasi-optical launch paths which can inject the microwave beams symmetrically either above or below the MAST-U midplane. These launchers are named delta (δ or D) and epsilon (ϵ or E), corresponding to the system's two gyrotrons, and consist of a focusing mirror (M1) and a steering mirror (M2). Sketches of the beam propagation through the δ (blue) and ϵ (insert, green) optics are drawn in figure 2, showing the expansion of the microwave beams as they propagate from the waveguide aperture through the mirror arrangement. All focusing mirrors in the quasi-optical systems presented here are created from ellipsoids of revolution, providing an input and output focal point. The one slight exception is DM1 which has a virtual output focal point behind the mirror surface. This enables the midplane δ launcher to inject power both in flat-top plasma operation and during start-up. The main constraints driving the design of the midplane launcher are as follows: the midplane port through which the beams are transmitted is currently an entry port for in-vessel access; therefore, the launcher assembly must be contained within the DN600 port area so as to be easily removable during machine shutdown for maintenance, restricting the mirror locations and dimensions. MAST-U's machine parameters dictate the chosen gyrotron frequencies, 28 and 34.8 GHz, which are lower than typical for microwave heating systems and so the optics here must accommodate the relatively greater beam divergence. As explained above, the steering mirrors must be on the midplane to provide balanced, zero net-current injection, which restricts their locations further. In addition, a wide angular steering range is required to cover these two main injection directions, so the M1s should ideally be positioned on a vector perpendicular to these two directions (the primary M2 rotation axis) in order to minimise the M2 dimensions. The steering mirrors should be flat to prevent potential astigmatism introduced by misalignment when steering a curved mirror, meaning the launcher focusing and coupling efficiency are dictated by the distance from the waveguide apertures to the corresponding M1s. An output beam waist of at least 6λ is targeted to achieve $\sim 90\%$ or greater coupling efficiency. Coupled with the requirement for each mirror to capture $\geq 99\%$ of the incident beam at 28 GHz, this drives the mirror dimensions to increase. The two waveguides enter the vacuum vessel port parallel and in a horizontal plane, so the M1s and M2s sit side by side, as can be seen in figure 1. In this CAD image the solid cones represent the 99% power beam diameter through the two mirrors and into the nominal co-current and counter-current plasma coupling windows. The translucent pink cones show the extents of the steering range in each main direction for optimal coupling to plasmas with a range of parameters and including $\pm 5°$ steering in the toroidal and poloidal axes. An equivalent set of output beam cones can be seen for the upper launcher which will be described in the following section.

B. Start-up launcher

One midplane launcher (δ) has a dual function to deliver high-field side injection during plasma start-up, following up on microwave-assisted start-up experiments on MAST [4] with 10-fold increases in power and beam pulse duration. A polariser grating tile is already installed on the centre column (CC) to reflect the injected O-mode into X-mode, which is

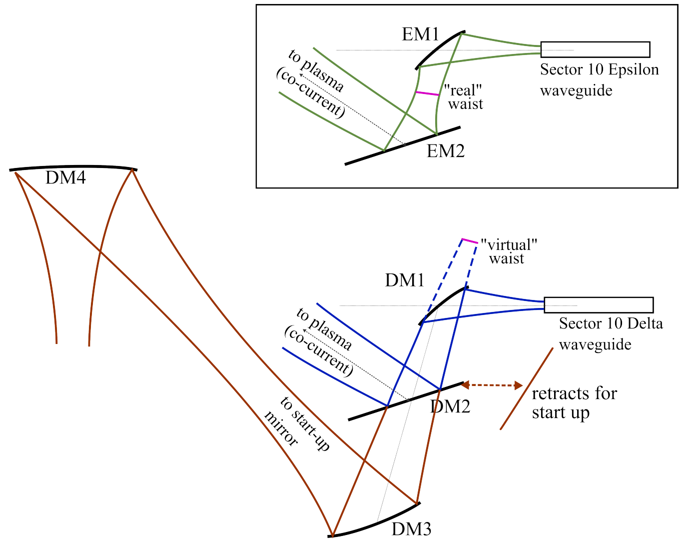

Fig. 2. Sketch of the on-axis launcher paths for the two gyrotron beams, Delta and Epsilon, showing the difference in focusing of the M1s and the alternate start-up operational mode for the Delta launcher (red). The mirrors and beams are effectively flattened onto a poloidal plane. The insert shows the epsilon beam profile (green) where EM1 is part of an ellipsoid of revolution surface to focus the beam onto the EM2 steering mirror. We designed DM1 as a modified ellipsoid of revolution, to give a "virtual" output beam waist behind its reflective surface, which matches the required delta beam (blue) radii at DM2 and DM3.

absorbed at the plasma resonance above the midplane, driving current parallel to that driven by the solenoid. To provide this capability while retaining as much efficiency and access during flat-top operation, we include the DM3 mirror underneath DM2, along the DM1-DM2 vector. The semi-transparent blue cones in figure 3 show the beam path of this alternative configuration of the 10δ launcher up to the CC polariser. The steering mirror DM2 is retractable towards the vessel port allowing the beam to pass to M3, which focuses the beam over 2.3 m onto M4, located in the machine sector containing the CC tile. The beam converges strongly from M4 onto the polariser tile, focusing $> 99.9\%$ of the incident power within the polariser pattern. The existing polariser grating was designed for 28 GHz, hence the midplane launchers operate at dual-frequency, with 34.8 GHz being the primary for flat-top current drive. As we sized each mirror to capture $\geq 99\%$ beam power at 28 GHz, more power is automatically captured at the primary frequency.

C. Off-axis / Upper launcher

The EBW upper launcher provides co-current injection only at approximately 600 mm above the MAST-U midplane. The two gyrotron beams enter the vacuum vessel in sector 9, adjacent to the midplane launchers in sector 10, through a DN250 port. We found no viable two-mirror optical layout for this launcher due to the spatial constraints of our 88.9 mm waveguide, beam expansion and other in-vessel components. Consequently, we have designed a four mirror configuration, similar to the TCV upper launcher [5], housing the first two mirrors in an additional vacuum chamber mounted onto the port. This facilitates key freedom in the waveguide routing

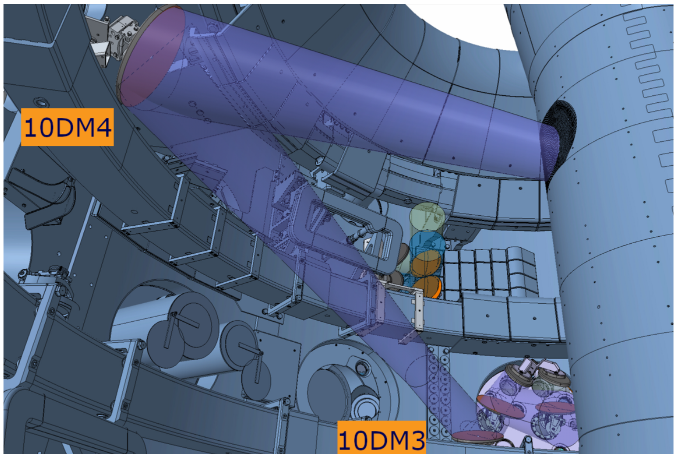

Fig. 3. An alternative configuration of the on-axis delta launcher for plasma start-up sends the beam, shown here by translucent blue cones, across the vessel to a grating polariser tile on the centre column. O-mode at 28 GHz is injected and converted on the high-field side into X-mode which is absorbed at the electron cyclotron resonance. The delta steering mirror (DM2) is retracted close to the port allowing the beam to pass through two focusing mirrors (DM3 and DM4) and onto the polariser, with a total path length of 4.5 m.

process to minimise the number of mitre bends, which are the predominant source of loss in the transmission line. Figure 4 shows a cartoon of the launcher layout, beam profiles and additional vacuum chamber and figure 5 shows the in-progress CAD of the launcher in the MAST-U vessel environment. We had to have M1s with sufficient focusing power to fit the beams through the port, as well as balance the separation of the M3s with the beam-port clearance. Due to the larger divergence of the 28 GHz beams we were unable to route them to the plasma, so the upper launcher will operate solely at 34.8 GHz. The translucent blue and green cones (δ and ϵ, respectively) in figure 5 show the beam paths through the four mirrors, which cross as they pass through the vacuum vessel port. The final beam sections into the plasma in this figure are shown as solid cones in figure 1, where the outer steering range encompassed by the semi-transparent pink cones is required to access different plasma scenarios, with the same $\pm 5°$ toroidal and poloidal steering about the optimum launch angles.

III. Midplane beam profiles and modelling

Here we include several figures of the midplane launcher envelope profiles, showing radii of the Gaussian beams throughout the launcher paths, simulated cross sections of the injected beams and comparisons of the simulated beam radii with analytical Gaussian beam propagation. Figure 6 shows the 99%-power radius of the δ beam at both frequencies (green lines) and the ϵ beam (pink lines). These radii are calculated for the designed frequency of 28 GHz using the analytical formula for Gaussian beam divergence, then the propagation of the 34.8 GHz beams is found using quasi-optical propagation matrices. Increased divergence with decreased frequency can clearly be seen when comparing the two gyrotron frequencies (solid and dashed lines). Virtual propagation from the DM1 output beam waists, located behind the mirror surface, are included as dotted lines. Generally, EBW coupling efficiency

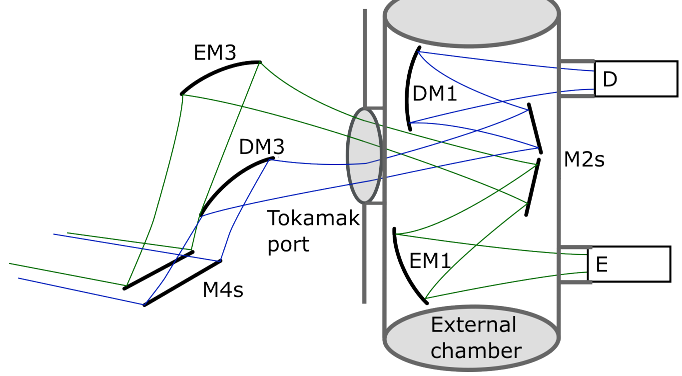

Fig. 4. Sketch of the off-axis launcher paths for the two gyrotron beams, Delta and Epsilon, showing the beam travelling right to left through the four mirror path between waveguide aperture and plasma. The first two mirrors in each path sit in an additional vacuum chamber mounted onto the tokamak vacuum vessel. Mirror pairs M1 and M3 are focusing while pairs M2 and M4 are flat. The M4s are steerable to direct the beams over a range of toroidal and poloidal injection angles.

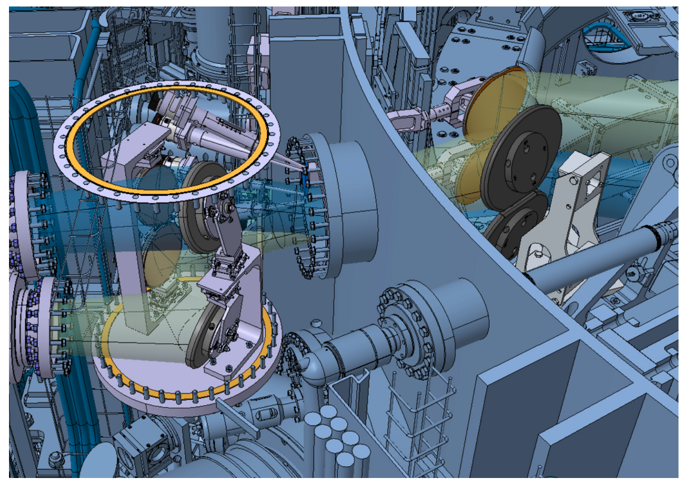

Fig. 5. Off-axis launcher assembly showing the delta (blue) and epsilon (green) beams entering the vacuum vessel from left to right. An ex-tokamak vacuum chamber (semi-transparent) is mounted to the main vessel port, containing the first two mirrors to focus and direct the beams through the DN250 port. The third and fourth mirrors focus and steer the beams into the plasma.

increases with increasing waist/wavelength ratio [1], so we have striven to keep the launcher output beam waists as large as possible. Our target waist/wavelength ratio was 6λ and we have achieved ratios of between 4.5 to 5.1 for the midplane launcher. As the upper launcher will only operate at the higher gyrotron frequency, we have achieved ratios of 5.6 and 6.0.

We cross-checked the analytical launcher optics with PROFUSION [6], modelling the quasi-optical beam propagation and calculate the cross-polarisation and higher-order mode content of the injected beams. Cross sections of the δ beam power density after M2 are shown in figure 7, showing the difference in divergence between the two frequencies. As less truncation occurs at 34.8 GHz the beam is less astigmatic than at 28 GHz, where the aperturing of $\sim 1\%$ power at each mirror introduces sufficient higher-order modes to the beam to be noticeable.

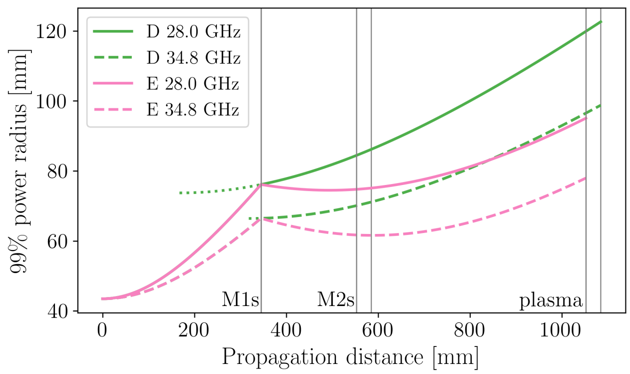

Fig. 6. Analytical beam envelopes (99% radii) for the midplane launchers at both 28 (solid) and 34.8 GHz (dashed) over the distance from waveguide aperture into the plasma. Mirror locations are shown by vertical grey lines. The green dotted lines show the beam profile from the virtual beam waists behind DM1 for both frequencies.

The astigmatism of both midplane beams can be seen in figure 8 by comparing the horizontal (subscript H) and vertical (subscript V) beam radii as the beams propagate from the M2s. These radii for the nominal co- and counter-current injection directions are compared against the analytical optics beam radii (the radii containing 99% of the beam power), for both launchers at 28 GHz. The ϵ beam exhibits greater discrepancies from the ideal than δ which is due to higher beam truncation, leading to a larger higher-order mode content and cross polarisation fraction. Similarly, the analytical and modelled beam radii for 34.8 GHz are plotted in figure 9. Again the propagation through both launchers shows acceptable agreement with the analytical design, with low astigmatism over the 2 m distance propagated past the steering mirrors, especially given the distance to the plasma is only 0.5 m. Some mirror steering positions lead to truncation of the beam within the 99% power contour, which will distort the injected beam and introduce more higher-order modes. We are in the process of quantifying these additional losses.

IV. In-vessel protection and diagnostics

In-vessel graphite tiles are required to protect components from uncoupled microwave power which is reflected from the plasma. The semi-transparent cones in figure 10 show the maximum possible extent of reflected beam coverage for all launch options. We are designing L-shaped tiles to sit over the main poloidal coils either side of the midplane (shown as semi-transparent grey in figure 1), and a combination of tiles will cover the upper launcher reflected beam area. The tiles will have textured surfaces to scatter the incident radiation and lower the peak power density, as well as preferentially direct power away from sensitive components and vacuum windows. We will monitor their temperature profiles with IR cameras, embedded and through-hole thermocouples to infer the microwave-plasma coupling efficiency. These diagnostics will also act as a fast interlock on the gyrotrons if the graphite temperature sees too sharp a temperature rise, indicating poor coupling and high reflected power.

V. Conclusion

In this article we have provided an update on the MAST-U EBW project optics and in-vessel component design requirements, engineering constraints and current status, along with expected performance from modelling and comparison to the analytical design. We have achieved the EBW launcher system requirements within the engineering and MAST-U environment constraints. The outcome is a system with high flexibility to enable a thorough study of EBW current drive, start-up and theoretical model validation with a view for impacting future tokamak heating and current drive systems.

Acknowledgments

This work has been part-funded by the EPSRC Energy Programme [grant number EP/W006839/1]. To obtain further information on the data and models underlying this paper please contact *publicationsManager@ukaea.uk*. The authors would like to thank the MAST-Upgrade team for their support and contributions, Burkhard Plaum and Carsten Lechte at IGVP Stuttgart for their valuable modelling and design work, Tim Goodman at EPFL for his insight and guidance on all things microwave, the ECRH team at ASDEX-Upgrade for helpful discussions and IDOM for their creative solutions to steer the EBW mirrors.

References

[1] Freethy, Simon, Figini, Lorenzo, Henderson, Mark, El-Haroun, Hana, Eliason, Bengt, Gibson, Sam, Kirov, Krassimir, Köhn-Seemann, Alf, Konoplev, Ivan, Saarelma, Samuli, Sharma, Ridhima, Speirs, David, Vann, Roddy, Webster, Helen, Wilson, Thomas, and the STEP team, "Microwave current drive for STEP and MAST Upgrade," *EPJ Web Conf.*, vol. 277, p. 04001, 2023. [Online]. Available: https://doi.org/10.1051/epjconf/202327704001

[2] H. Webster, S. Freethy, M. Henderson, J. Allen, O. Caretta, S. Desai, J. Holden, D. Maszczyk, E. Melidis, H. Meyer, E. Muir, A. Munasinghe, and S. Surendran, "MAST upgrade microwave heating and current drive system – engineering design overview," *EPJ Web of Conferences*, vol. 277, p. 04004, 2023. [Online]. Available: https://doi.org/10.1051/epjconf/202327704004

[3] H. Webster, S. Freethy, M. Henderson, J. Allen, O. Caretta, S. Desai, E. Melidis, H. Meyer, E. Muir, A. Munasinghe, and S. Surendran, "Design and Development of an Electron Bernstein Wave Heating and Current Drive System for MAST-U," *(IAEA FEC 2023 contribution number IAEA-CN-316/2386)*, 2023.

[4] V. Shevchenko, Y. Baranov, T. Bigelow, J. Caughman, S. Diem, C. Dukes, P. Finburg, J. Hawes, C. Gurl, J. Griffiths, J. Mailloux, M. Peng, A. Saveliev, Y. Takase, H. Tanaka, and G. Taylor, "Long pulse EBW start-up experiments in MAST," *EPJ Web of Conferences*, vol. 87, p. 02007, 2015. [Online]. Available: https://doi.org/10.1051/epjconf/20158702007

[5] T. Goodman, S. Alberti, M. Henderson, A. Pochelon, and M. Tran, "Design and installation of the electron cyclotron wave system for the TCV tokamak," in *Fusion Technology 1996*, C. VARANDAS and F. SERRA, Eds. Oxford: Elsevier, 1997, pp. 565–568. [Online]. Available: https://www.sciencedirect.com/science/article/pii/B9780444827623501117

[6] B. Plaum, "Simulation of microwave beams with profusion," Universität Stuttgart, Tech. Rep., 2022. [Online]. Available: http://elib.uni-stuttgart.de/handle/11682/12258

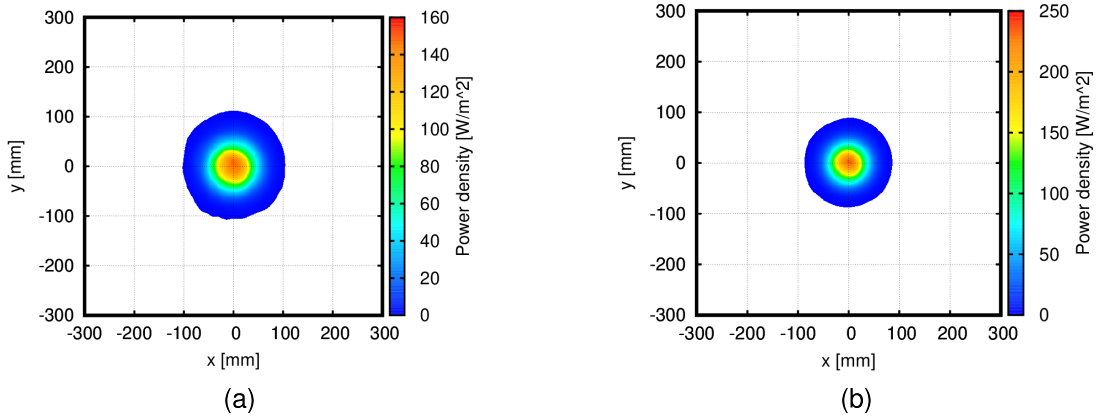

Fig. 7. Beam power density cross sections 200 mm after the 10δ steering mirror at 28 GHz (a) and 34.8 GHz (b) for an input beam power of 1 W, modelled in PROFUSION [6]. The profiles are close to circular and the outer contour shown contains 99% of the Gaussian beam power, i.e. the $3w$ beam diameter.

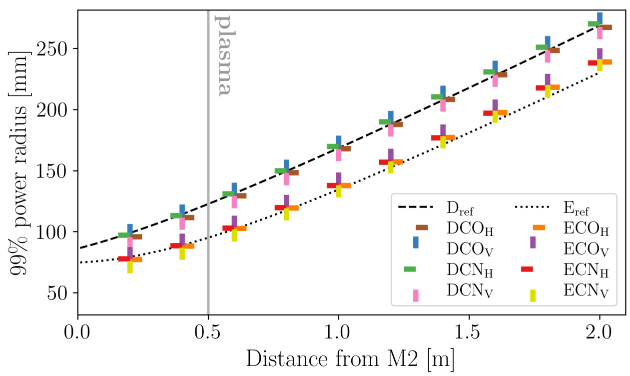

Fig. 8. Propagation after the midplane DM2 and EM2 steering mirrors: a comparison of analytical beam envelope against simulated beam propagation in PROFUSION at 28 GHz, plotted are the radii containing 99% of the beam power. Data is shown for orthogonal axes (**H**orizontal and **V**ertical subscripts) of the beams in the nominal co- (CO) and counter-current (CN) steering directions. The vertical grey dotted line shows the average distance to the plasma (0.5 m) over the range of plasma scenarios.

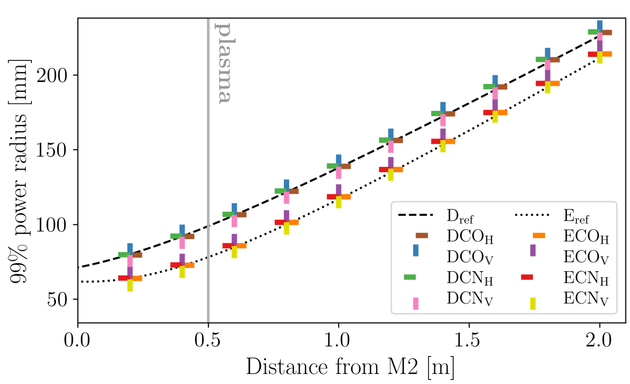

Fig. 9. Propagation after the 10DM2 and 10EM2 steering mirrors: comparison of analytical beam envelope against simulated beam propagation in PROFUSION at 34.8 GHz, values are the radius containing 99% of the beam power. Data is shown for orthogonal axes (**H**orizontal and **V**ertical subscripts) of the beams in the nominal co- (CO) and counter-current (CN) steering directions. The vertical grey dotted line shows the average distance to the plasma (0.5 m) over the range of plasma scenarios.

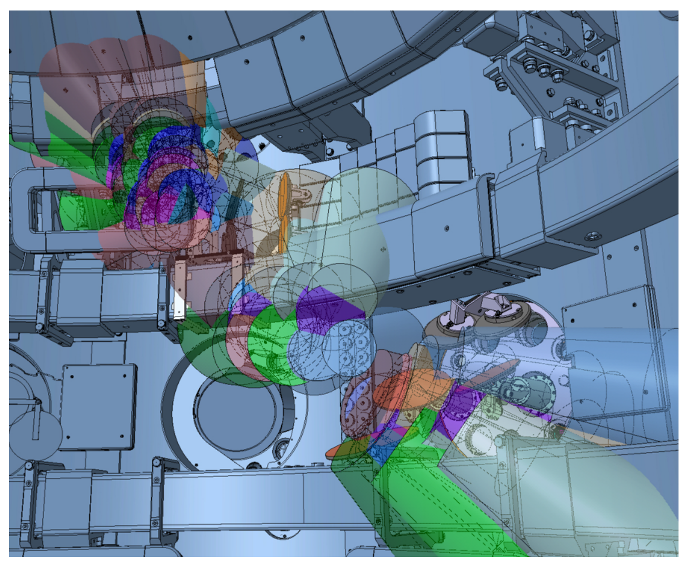

Fig. 10. Reflected beam cone models for the midplane and upper launchers showing the extremities of the possible area un-coupled, reflected power may land over the range of steering mirror injection angles.